photochem

MDPI

Review

Recent Advances in Aerobic Photo-Oxidation over Small-Sized IB Metal Nanoparticles

Yifei Zhang [1,2], Meng Wang [3,*] and Gao Li [2,*]

[1] Institute of Catalysis for Energy and Environment, College of Chemistry and Chemical Engineering, Shenyang Normal University, Shenyang 110034, China; sszyf2017@126.com
[2] State Key Laboratory of Catalysis, Dalian Institute of Chemical Physics, Chinese Academy of Sciences, Dalian 116023, China
[3] Key Laboratory of Biofuels and Biochemical Engineering, SINOPEC Dalian Research Institute of Petroleum and Petro-Chemicals, Dalian 116045, China
* Correspondence: wangmeng.fshy@sinopec.com (M.W.); gaoli@dicp.ac.cn (G.L.)

Abstract: Aerobic photo-oxidation is a kind of green catalytic process that give valuable chemicals because of its mild reaction conditions and high product selectivity. Recently, small-sized IB metal nanoparticles (NPs; e.g., Cu, Ag, and Au, sized 1–3 nm) upon the surface of titanium oxide show excellent photocatalytic performance. The introduction of IB metal NPs can enhance the separation of photo-generated holes/electrons during photo-oxidations. In this account, we summarize the recent progress of small-sized IB metal NPs catalyzed by aerobic photo-oxidations, including the conversion of methanol, ethanol, sulfide, and benzylamine. More importantly, the structure–property correlations at the atomic level are detailed and discussed, e.g., the insights into the activation of oxygen and the identification of catalytic active sites. Future investigations are needed to carry out and reveal the catalytic mechanisms and conversion pathways.

Keywords: IB metal; 1–3 nm; structure–property correlations; nanoclusters; photo-oxidation

Citation: Zhang, Y.; Wang, M.; Li, G. Recent Advances in Aerobic Photo-Oxidation over Small-Sized IB Metal Nanoparticles. *Photochem* **2022**, *2*, 528–538. https://doi.org/10.3390/photochem2030037

Academic Editor: Ewa Kowalska

Received: 22 June 2022
Accepted: 11 July 2022
Published: 13 July 2022

1. Introduction

In recent decades, well-defined IB metal nanoclusters (NCs) have been documented as novel and promising model catalysts owing to their unique electronic configuration [1–5]. For example, Au/Ag NCs show intrinsically different catalytic behaviors in comparison with conventional gold or silver nanoparticles (Au/Ag NPs) [6–10], which results in superior catalytic properties in many organic reactions, such as selective oxidation and hydrogenation and carbon-carbon couplings. Furthermore, the metal NCs with a nanometric size (1–2 nm) exhibit a non-metallic property with energy quantization manifested in their HOMO–LUMO gap, which is opposite to the localized surface plasmon resonance (LSPR) of conventional metal NPs [11,12]. The electron of the Au/Ag NCs can be excited from HOMO to LUMO upon illumination, resulting in the generation of electron/hole pairs as the semiconductors. The generation and subsequent recombination of the electron/hole pairs using solar energy are of great interest for photocatalytic and photovoltaics applications. Therefore, the catalytic activity of Au/Ag NCs has been demonstrated in solar energy harvesting for power production and the photocatalytic degradation of pollutants [13,14].

TiO_2-based semiconductors have been well documented in photo-oxidations [15–17]. Recently, supported small-sized CuO_x NPs (3–5 nm), with a high population of surface oxygen vacancies, have been applied in a serial of redox reactions [18–21]. Firstly, these CuO NPs can aid the minimizing recombination of photo-generated electrons/holes, thus improving the photocatalytic activity. Secondly, the supported CuO_x NPs can offer a unique electronic structure and synergistic effects, promoting photocatalytic reactions that occur at the interface of the photocatalysts. Therefore, the nanocomposites comprised of CuO NPs and TiO_2 semiconductors should be a good candidate for photocatalytic oxidation reactions.

Herein, we introduce the recent progress of photocatalytic transformations for valuable chemical productions, including the aerobic photo-oxidation of methanol to methyl formate over small-sized CuO supported onto TiO_2 in the gas phase, and the photocatalytic conversions of ethanol, sulfide, and benzylamine over Au/Ag NC photocatalysts, mainly in our lab until May 2022. Moreover, the extrapolate reaction pathways and tentative catalytic mechanisms, by density functional theory (DFT) studies, are detailed and discussed based on the systems developed.

2. Methanol Conversion to Methyl Formate

Methyl formate is one of the important chemicals applied in synthesis intermediates, the solvent for cellulose, and fumigants and fungicides [22–26]. The anatase-TiO_2 was shown to be a poor photocatalyst [27,28]; thus, the CuO/anatase-TiO_2 system was developed [29]. The previous studies only focused on titanium dioxide with mixed crystals (e.g., P25) as the support, which is not feasible to study the mechanism and the interaction of TiO_2 supports and metal NPs. Note that the interfacial perimeter of the oxide supports and metal NPs is often deemed as the catalytically active sites during the metal NPs catalyzed reactions.

In past decades, the well-defined anatase-TiO_2 with different shapes (such as rods, sheets, spindles, tubes, etc.) has been prepared [30,31]. TiO_2 has specific exposing facets; for example, TiO_2{001} and TiO_2{101} surfaces are observed in the TiO_2-sheet sample (Figure 1a), which have been widely used as photocatalysts [32,33]. The CuO/TiO_2-sheet photo-catalyst was prepared via a reduction-deposition method and used for the methanol photo-oxidation to methyl formate by oxygen (O_2) [26]. The CuO particles of ~3.5 nm were found to be supported on the TiO_2{101} facet of the TiO_2-sheet. The CuO species can greatly reduce the recombination of photo-generated electrons/holes under light irradiation. The CuO/TiO_2 sheet exhibited excellent performance under mild conditions for the catalytic photo-oxidation of methanol. The activity of the CuO/TiO_2-sheet was improved by increasing the reaction temperatures, and the methyl formate selectivity decreased simultaneously.

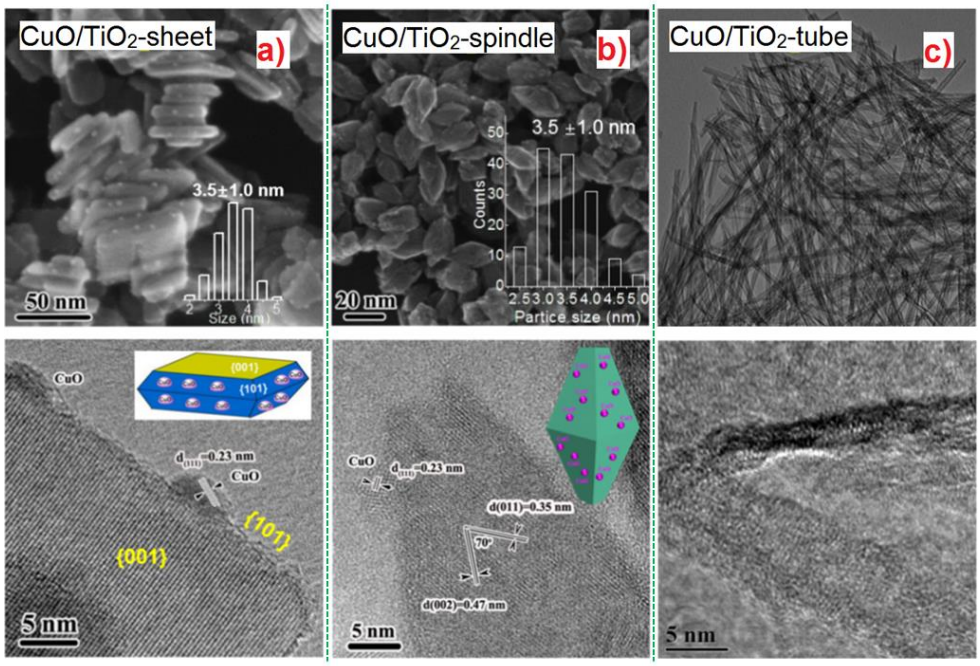

Figure 1. TEM images of the CuO/TiO_2 with different morphologies: (**a**) TiO_2-sheet, (**b**) TiO_2-spindles, and (**c**) TiO_2-tube. Reproduced with permission from Refs. [26,34,35]. Royal Society of Chemistry, 2019. Springer, 2020, and American Society of Chemistry, 2020.

The further investigation focused on the concentration of the CuO_x-loading when the conversion of a nearly 95% selectivity for methyl formate was larger than 85% could be reached with the CuO_x/TiO_2 photocatalyst; this was the best result in our reaction system (Figure 2). More CO_2 could be found when the concentration of O_2 increased to 0.75% and 1.0%, so 0.5% O_2 should be the most suitable choice by considering both the conversion and selectivity. At room temperature and optimal conditions, the reaction rate for methyl formate production can reach up to 10.8 mmol g^{-1} h^{-1}, which is much higher than the used bare CuO_x oxides or only a TiO_2-sheet. After a reaction for 20 h, the CuO_x/TiO_2-sheet nanocomposites still could show excellent catalytic activity. The synergistic effects and unique electronic structure were considered to be the main reasons for their superior catalytic activity.

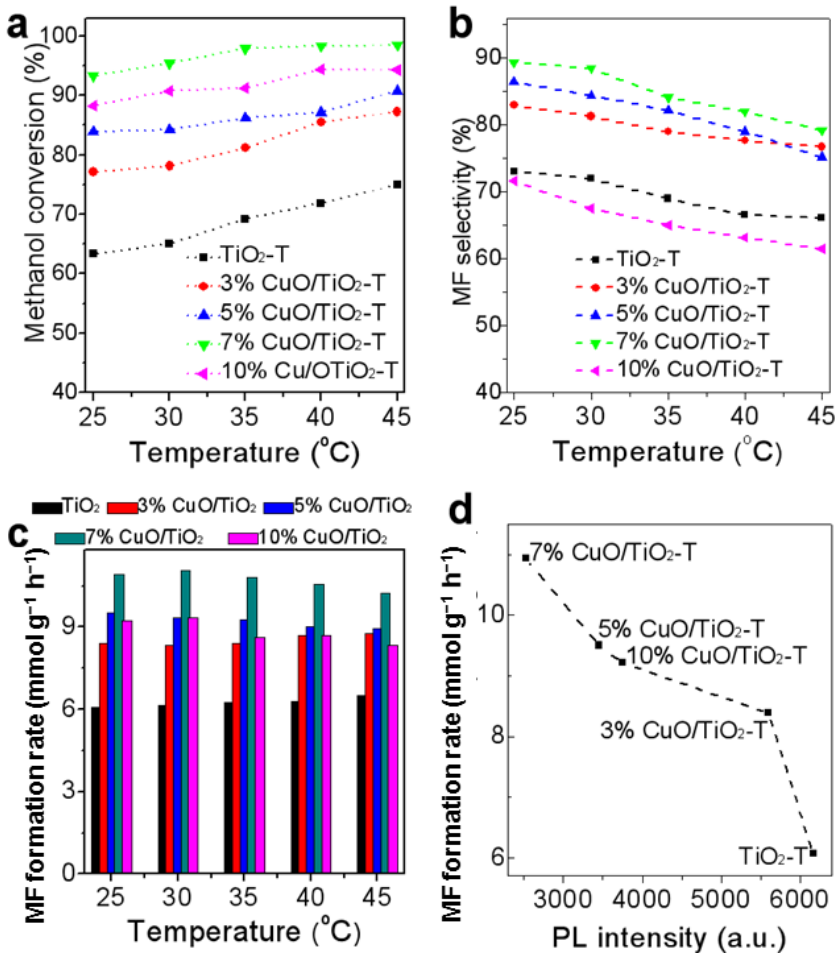

Figure 2. (**a**) CH_3OH conversion, (**b**) MF selectivity, and (**c**) MF formation rate as a function of temperature over nanocomposites. (**d**) Relationship between PL intensity and MF formation rate. Reproduced with permission from Ref. [35]. American Society of Chemistry, 2020.

In the following investigation, Shi et al. supported the CuO_x nanoclusters on the side of the TiO_2{101} plane of a TiO_2-spindle (Figure 1b) [34]. It is necessary to mention that CuO_x nanoclusters could not be anchored on the top of the TiO_2-spindle because there was not enough space. As a result, CuO/TiO_2 is a kind of excellent candidate for methanol oxidation; a conversion of >97% and 83% selectivity could be obtained under mild reaction conditions. Further investigation revealed that the presence of surface oxygen vacancy (O_V) species is an important factor for catalytic activity in the CuO/TiO_2-spindle catalyzed reactions [35]. Thus, the catalytic activity of small-sized CuO nanoparticles could be improved by tuning the excitons' recombination with O_V generation.

Further, for the first time, in-situ attenuated total reflection infrared (ATR-IR) spectroscopic analysis reveals that the adsorbed methoxy (CH_3O*) was converted to an adsorbed formaldehyde (CHO*) species in the presence of oxygen in the methanol conversion (Figure 3a). The methyl formate was formed by a CHO* species that further reacted with a neighboring CH_3O* [34]. The reaction mechanism with the CuO/TiO_2 catalysts is shown in Figure 3b. With UV irradiation, electrons are formed at the $TiO_{2'}$s valence band and further transferred to its conduction band, coming out of the holes and electrons. Then, the accumulated electrons are transferred to the surface of CuO by a p-n heterojunction, which accelerates the separation speed of photo-generated electrons and holes, obviously, and the holes with positive charges could promote the formation of HCHO* formation by CH_3OH oxidation. A dissociation of oxygen occurred over the CuO particles with the aid of the generated electrons to refill the TiO_2 oxygen vacancies, which are the rate-determining steps during the methanol photo-oxidations [35].

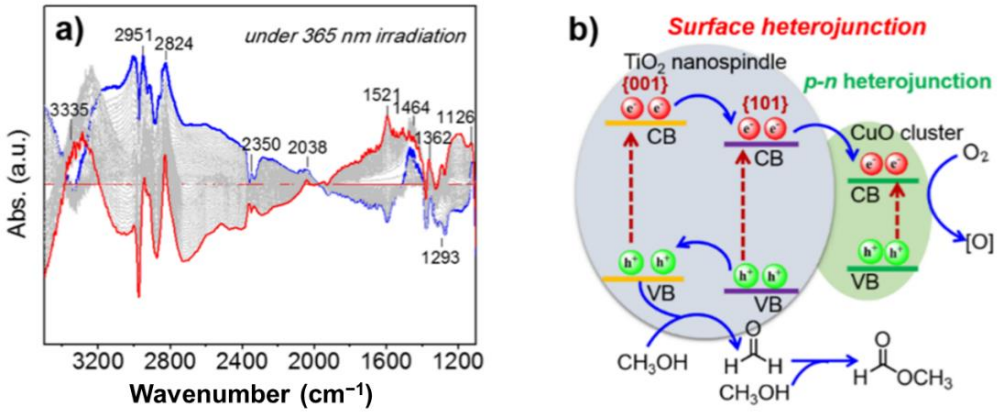

Figure 3. (**a**) ATR-IR monitoring of CuO/TiO_2 under 365 nm of light. (**b**) Proposed mechanism. Reproduced with permissions from Ref. [30]. Springer, 2019.

3. Ethanol Conversion

C9-C13 bio-fuels synthesized from cellulosic ethanol oxidation with cinnamaldehyde in a liquid have been well catalyzed by the nanogold particles supported by metal-oxides [35]. In a one-pot cascade cross aldol condensation reaction by K_2CO_3 as the cocatalyst, the Au/NiO catalyst could achieve a selectivity as high as 70% for C11-C13 hydrocarbon [36]. At the sites of NiO oxide's oxygen vacancies, ethanol was transformed into acetaldehyde (CH_3CHO*), which can be testified by EtOH-TPD and TGA analyses. Then, the reaction of cinnamaldehyde with CH_3CHO* happened at the interfacial perimeter of the Au/NiO composite through the cascade reactions. The whole catalytic process was investigated by in-situ infrared spectroscopy.

Atomically precise metal nanoclusters with certain structures also have been used in catalytic selective oxidations as a kind of well-defined model nanocatalyst [37–39]. Their electronic property could be tuned by mono-dopant into a metal particle at a specific position and thus change their catalytic activity. Qin et al. reported a method to dope a mono-Ag-atom at the central site of $Au_{13}Ag_{12}(PPh_3)_{10}Cl_8$ nanoclusters with a rod-shape and finally prepared a new kind of "pigeon-pair" cluster, which is called $\{[Au_{13}Ag_{12}(PPh_3)_{10}Cl_8]\cdot[Au_{12}Ag_{13}(PPh_3)_{10}Cl_8]\}^{2+}$ [40,41]. The single-atom exchange between nanoclusters with the same structure resulted in an obvious disturbance to the electronic characters, which could lead to a difference in catalytic performance [42–44]. In order to investigate the influence of a single-atom exchange in the catalytic reaction, $Au_{13}Ag_{12}$ and $Au_{13}Ag_{12}.Au_{12}Ag_{13}$ clusters were both supported on TiO_2 and used in the photocatalytic conversion of ethanol [45]; the reaction proceeded under a UV irradiation at 30 °C. As can be seen from Figure 4, $Au_{13}Ag_{12}\cdot Au_{12}Ag_{13}$ clusters achieved a higher conversion of ethanol, which is about 1.5-fold compared with the $Au_{13}Ag_{12}$ clusters (23%), and the selectivity of ethanal for the $Au_{13}Ag_{12}\cdot Au_{12}Ag_{13}$ clusters (79%) is slightly higher

than the $Au_{13}Ag_{12}$ clusters (72%). Because the product distribution is very similar for the two different clusters, it could be concluded that the catalytic reaction mechanism and the conversion pathway over both catalysts should be the same. In brief, the single-atom exchange from Au to Ag in the same structure of the M_{25} clusters leads to a significant difference in the catalytic activity caused by distinct electronic properties.

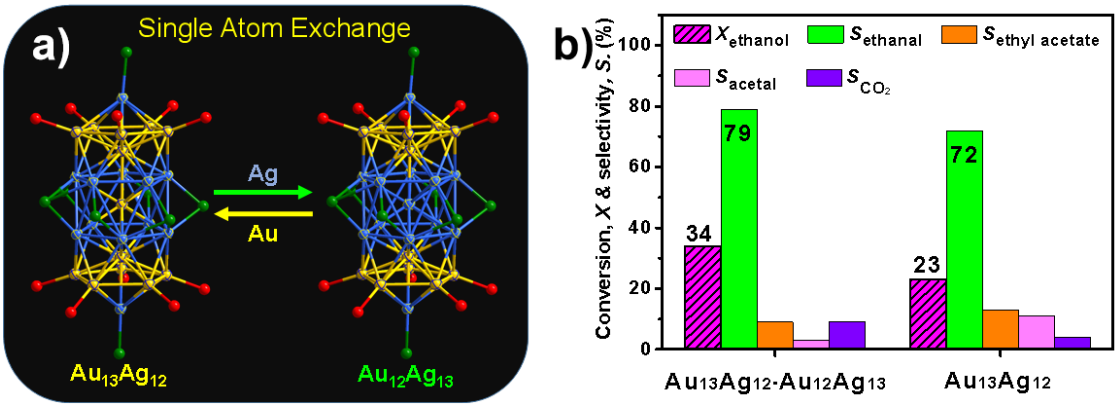

Figure 4. (**a**) Metal exchanging at the central site of the M25 clusters. (**b**) Photocatalytic performance in the ethanol conversion. Reproduced with permission from Ref. [46]. Springer, 2022.

4. Benzylamine to Imine

The catalytic selective oxidation of amines to corresponding imines is a kind of significant and important reaction due to the extensive applications in the industry of fine chemicals and pharmaceuticals [47]. Tada and coworkers reported a plasmonic gold photocatalyst which gave a 4.5% conversion of benzylamine to imine without a solvent [48]. The metal clusters show a good capacity to adsorb UV/VIS lights [49,50]. With the aim to expand the application of support for Au nano-cluster catalysts in this reaction system, we anchored $[Au_{25}(PPh_3)_{10}Cl_2(SR)_5]^{2+}$ rods with a HOMO-LUMO gap of ~1.84 eV ($>\Delta E_{act}$) on a P25 (mixed anatase and the rutile phase of TiO_2) to obtain Au_{25}/P25 nanocomposites with ligands intact on the cluster's surface and used it in the photo-oxidation of benzylamine under visible light ($\lambda \approx 455$ nm) in the presence of O_2 [51]. After 2 h of light irradiation, the conversion was 82% with the Au_{25}/P25, which is much higher than bare P25 (about 14%) in the same reaction conditions. After three times of cycle use, only a 10% decrease in activity happened, and the selectivity was still maintained at >99%.

Figure 5b shows a plausible catalytic reaction mechanism; under light irradiation, Au_{25} rods could act as a narrow band gap semiconductor and lead to the separation of the holes and electrons. After being generated in the Au_{25} clusters by photo-oxidation, electrons could be transferred into the conduction band of P25 and react with O_2 to form O_2^-. Because the LUMO energy of Au_{25} is higher than that of the conduction band of P25 (−0.63 V to −0.9 V), the electrons could inject into the conduction band of P25 from Au_{25}. Firstly, on the surface of the nanocluster, α-H in the benzyl amine radical cation can be plucked by a Au atom without an organic ligand. By inducing amines, the phosphine ligands could be partially removed from the Au atoms; this process has been proved by experiment and theoretical calculations [52,53]. As a result, a Au-H intermediate, along with a carbocation intermediate, would be formed. The H atom could be withdrawn from the Au-H and amine by the O_2^- species to form PhCH = NH and H_2O_2. The benzyalamine would be oxidized by H_2O_2 to produce water and benzaldimine, which would undergo a nucleophilic attack by benzylamine to form aminal lately. Finally, the aminal group eliminates ammonia to produce an imine product.

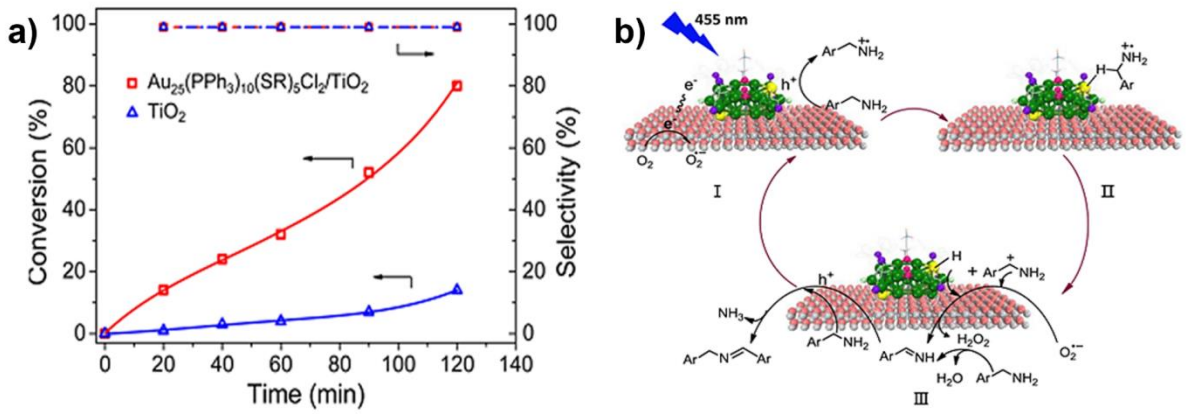

Figure 5. (**a**) Time-dependent catalytic activities of Au_{25}/P25 and P25 in the photo-oxidation of benzyl amine. (**b**) Mechanistic process of photo-oxidation. Reproduced with permission from Ref. [52]. Copyright 2017 American Chemical Society.

In a further experiment, a highly photostable novel alloy $Au_8Ag_3(PPh_3)_7Cl_3$ cluster (E_g~1.67 eV) was used in the photo-oxidation of benzyl amine to *N*-(phenylmethylene) benzenemethanamine under an LED light ($\lambda > 455$ nm) with the presence of O_2 at room temperature, Figure 6 [54]. The catalytic activity was also compared with its common monometallic counterpart, $Au_{11}(PPh_3)_7Cl_3$ (Eg~2.06 eV). Both the Au_8Ag_3/P25 and Au_{11}/P25 (0.5 wt.% cluster loading) were used without organic ligand removal. At the same reaction conditions, Au_8Ag_3/P25 had a 72.5% conversion compared with Au_{11}/P25, which only had a 37.8% conversion, and the selectivity for both was >99%. The turnover frequency for Au_8Ag_3/P25 was about two times higher than Au_{11}/P25 (1.51 s^{-1}); this could be attributed to the special electronic properties of the Ag_8Au_3 alloy cluster caused by the synergic effects from the Au and Ag atoms. A DFT investigation further revealed that Ag dopants in the C_3-axis delocalized the electrons of Au into the orbitals of the phosphorus atom and induced a disturbance in the electronic properties, which could affect the catalytic activity. It is worth noting that the reaction could not happen without light irradiation.

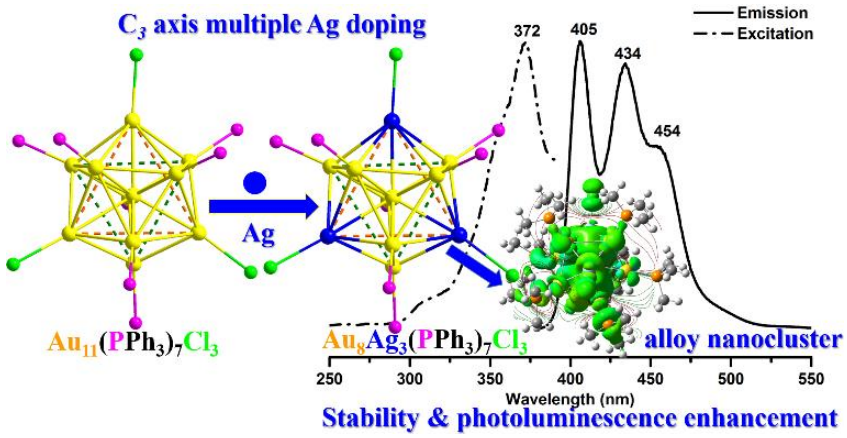

Figure 6. Fabrication of $Au_8Ag_3(PPh_3)_7Cl_3$ for the photocatalytic conversion of benzylamine to imine. Reprinted from Ref. [54]. Copyright 2019 Royal Society of Chemistry.

5. Sulfide to Sulfoxide

Singlet oxygen ($^1O_2$) is a kind of excited state of molecular oxygen ($^3O_2$ or triplet oxygen, i.e., a ground state). Because of its high reactivity, $^1O_2$ could take part in various kinds of chemical and biological reactions. However, according to the selection rule, the direct conversion between $^3O_2$ and $^1O_2$ spin states via photons' adsorption/emission is spin-forbidden [55]. In order to solve this issue, the photosensitizers (photo-absorbing

molecules) are usually used for the photo-mediated generation of $^1O_2$, which have to satisfy that the energy difference between the triplet and ground state of the photosensitizer (ΔE_t) should be larger than the activation energy of the triplet oxygen ($^3O_2$ to $^1O_2$ with $\Delta E_{act} \approx 0.97$ eV). Interestingly, different from metal nanoparticles, the metal nanoclusters with atomically precise structures exhibit HOMO-LUMO gaps (E_g) and $Au_{25}(SR)_{18}$, $Au_{38}(SR)_{24}$, and $Au_{99}(SR)_{42}$ clusters have an E_g of ~1.3, 0.9, and 0.71 eV, respectively [56]. So, Kawasaki et al. demonstrated the fact that the HOMO-LUMO gap (~1.3 eV > ΔE_{act}) of $Au_{25}(SR)_{18}$ permits it to be used in the production of $^1O_2$ [57]. The formation of $^1O_2$ through photo excitation with a cluster of such type ultimately leads to the transformation of various organic compounds. Mechanistically, the photo-excited sensitizer passed on its excess energy to $^3O_2$ to generate $^1O_2$, and the photosensitizer regenerated in the ground state without any consumption. Additionally, some superoxide ($O^{2\cdot-}$) and hydroxyl radicals ($^{\cdot}OH$) may also be formed at the same time via other photochemical reactions, such as an electron transfer process [58]. Next, these kinds of phenomena will be explained by demonstrating some of the key examples from our lab.

A novel structure called the $Au_{38}S_2(SAdm)_{20}$ cluster (size ~1.5 ± 0.3 nm) with a HOMO-LUMO gap of 1.57 eV (>ΔE_{act}) was found to be much more efficient at generating $^1O_2$ under a laser light of 532 and 650 nm [59]. As can be seen from Figure 7, the reaction mechanism involves a Dexter-Type electron exchange coupling between the excited photo-sensitizer and the ground state $^3O_2$ molecules. Briefly, the $Au_{38}S_2(SAdm)_{20}$ cluster was stimulated from its ground state (S_0) to an excited state (S_1) by photo excitation, then converted to a slightly lower energy state (T_1) with spin flipping via an intersystem crossing (ISC). $Au_{38}S_2(SAdm)_{20}$ in the ground state and the much-required $^1O_2$ could be generated by an electron exchange between the triplet state (T_1) of the $Au_{38}S_2(SAdm)_{20}$ cluster and $^3O_2$.

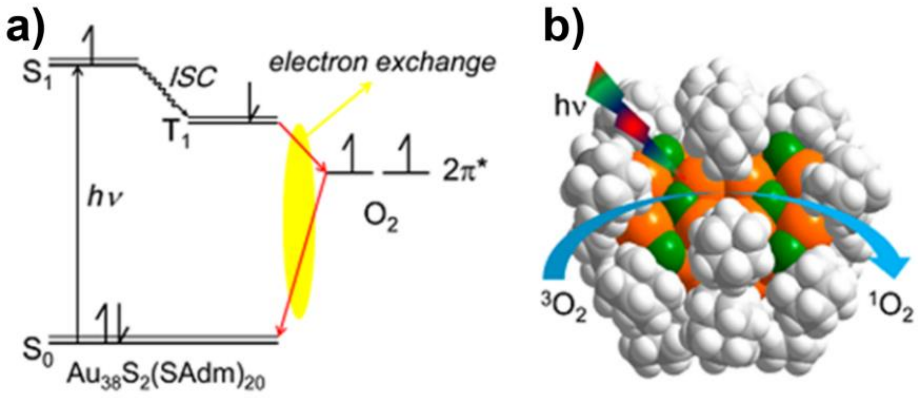

Figure 7. (**a**) Mechanism of the Dexter-Type electron exchange for $^1O_2$ generation. (**b**) Description of the generation process. Reprinted with permission from [59]. Copyright 2017 American Chemical Society.

Then, the $Au_{38}S_2(SAdm)_{20}$ cluster was further used for photocatalytic sulfoxidation reactions in an open quartz vessel with O_2 bubbling under light irradiation (λ = 532 nm). As earlier reported, gold nanoclusters could display excellent catalytic performance in the selective oxidation of sulphides to sulfoxides using a chemical oxidant, e.g., PhIO (without any light irradiation), and this reaction system results in over-oxidized impurities, such as sulfones [60]. Photocatalytic sulfoxidation with molecular oxygen as the oxidant is more economical and environmentally friendly.

It is worth noting that no catalytic activity could be observed in the absence of light; under light at λ ≈ 532 nm, the catalytic activities of the $Au_{25}(SR)_{18}$ and $Au_{38}S_2(SAdm)_{20}$ clusters could achieve up to 18% and 57%, with 100% selectivity for methyl phenyl sulfoxide. After three reaction cycles, no loss of catalytic activity and selectivity for $Au_{38}S_2(SAdm)_{20}$ was observed. The high efficiency of the $^1O_2$ generation with $Au_{38}S_2(SAdm)_{20}$ prompted the further investigation of the photocatalytic activity of the $Au_{38}S_2(SAdm)_{20}$ nanoclusters used in a one-step selective chemical transformation of benzylamine to

N-(phenylmethylene)benzenemethanamine under an LED light ($\lambda \approx 455$ nm) in the atmosphere of O_2. In the same reactions, a 99% conversion of the substrate was reached in 0.5 h with >99% selectivity; this result is much better than supported Au nanoparticles (6–12 nm) [61]. As expected, the catalytic activity for the $Au_{38}(PET)_{24}$ clusters, with a HOMO-LUMO gap of ~0.9 eV ($<\Delta E_{act}$), decreased sharply (only by ~20% in the benzylamine conversion); it obviously indicates that the high catalytic conversion (99%) of $Au_{38}S_2(SAdm)_{20}$ is due to the formation of a singlet $^1O_2$ during the photocatalytic reaction. Importantly, part of the photocatalytic oxidation caused by the Au nanoclusters should also happen via the electron transfer process and the production of the benzyl amine cation.

Next, the $[Au_{13}(dppe)_5Cl_2]^{3+}$ (Au_{13}) NC with a propeller-like structure and a HOMO-LUMO gap of ~1.9 eV had a high $^1O_2$ quantum yield of 0.71 [62], which is considerably close to that of anthracene. Of note, the Au_{13} NCs were intact and stable during the $^1O_2$ generation.

6. Conclusions, Challenges, and Future Perspective

In summary, high valuable chemical products synthesized by aerobic photocatalytic oxidation with supported IB metal nanoclusters have been fabricated in this study; some significant breakthroughs are summarized below:

(1) Four different types of photo-oxidations were achieved over the TiO_2-supported metal nanoclusters and nanoparticles presented in this paper, including the photo-oxidation of methanol to methyl formate, and ethanol conversion, a benzylamine to imine conversion, and sulfide to sulfoxide conversion, which give some new exploits in photocatalysis.

(2) Copper oxide nanoclusters supported onto the TiO_2 semiconductors with a different morphology of nanosheets, nanospindles, and nanotubes have been prepared to investigate the performance of photocatalytic oxidation reactions. The morphology (exposed facets) effects have been well studied.

(3) The active centre for photocatalytic aerobic oxidation was identified and created as an example. The $CuO_x/TiO_2\{101\}$ interface was considered to be a key point in the photo-oxidation of methanol.

(4) Single-atom-exchanging in the metal clusters has a big influence on the catalytic activity but cannot affect product selectivity. However, the detailed mechanism is still unable to reveal this.

(5) Via the characterization of ATR-IR spectra to dig out the possible reaction intermediates [63], we have clearly mapped out the whole conversion pathway and worked out the controversy in this photocatalysis.

However, there are still some following points for utmost consideration:

(1) More efforts must be put into the creation of novel photo/catalysts with specific active reaction sites for a high-efficient conversion [64–66], and the catalytic efficiency should be further enhanced by the design of the novel metal nanoclusters or nanoparticles on other light-absorbing nanomaterials (e.g., ZnO, g-C_3N_4, BiOX, Mxenes, etc.). The photocatalysis also needs to be developed using UV/VIS light, which is close to the real applications.

(2) In order to reveal the reaction mechanisms, DFT studies and in-situ characterizations should be used in this catalytic reaction system, and, in turn, it will be more helpful in obtaining new photocatalysts with high efficiency.

(3) The photo-oxidation reactions should be further coupled with a thermal and electro method to improve the catalytic activity, which needs to develop a new type of photocatalyst [67–72].

(4) Alloy metal nanoparticle catalysts still need to be further and wildly used in catalytic biomass conversions; as the electronic property can be well modified to tune the catalytic performance, it is a kind of excellent method for designing suitable catalysts.

Author Contributions: Investigation, Y.Z. and M.W.; resources, Y.Z. and M.W.; writing—original draft preparation, Y.Z., M.W. and G.L.; writing—review and editing, G.L.; supervision, G.L.; project administration, M.W. and G.L. All authors have read and agreed to the published version of the manuscript.

Funding: We gratefully acknowledge the financial support from the Innovation Foundation of Dalian Institute of Chemical Physics (DMTO201802).

Institutional Review Board Statement: The study was conducted in accordance with the Declaration of Helsinki and approved by the Institutional Review Board.

Informed Consent Statement: Not applicable.

Conflicts of Interest: The authors declare no conflict of interest.

References

1. Jin, R.; Li, G.; Sharma, S.; Li, Y.; Du, X. Toward Active-Site Tailoring in Heterogeneous Catalysis by Atomically Precise Metal Nanoclusters with Crystallographic Structures. *Chem. Rev.* **2021**, *121*, 567–648. [CrossRef]
2. He, W.; Ma, G.; Shen, Q.; Tang, Z. Engineering Gold Nanostructures for Cancer Treatment: Spherical Nanoparticles, Nanorods, and Atomically Precise Nanoclusters. *Nanomaterials* **2022**, *12*, 1738. [CrossRef]
3. Yin, C.; Liu, S.; Qin, Z.; Zhang, Y.; Li, G.; Zhao, Z. Butterfly-Like Tetranuclear Copper(I) Clusters for Efficient Alkyne Homocoupling Reactions. *Eur. J. Inorgan. Chem.* **2021**, 392–397. [CrossRef]
4. Yao, Q.; Zhang, Q.; Xie, J. Atom-Precision Engineering Chemistry of Noble Metal Nanoparticles. *Ind. Eng. Chem. Res.* **2022**, *61*, 7594–7612. [CrossRef]
5. Li, G.; Jin, R. Atomically precise gold nanoclusters as new model catalysts. *Acc. Chem. Res.* **2013**, *46*, 1749–1758. [CrossRef] [PubMed]
6. Liu, L.; Corma, A. Metal Catalysts for Heterogeneous Catalysis: From Single Atoms to Nanoclusters and Nanoparticles. *Chem. Rev.* **2018**, *118*, 4981–5079. [CrossRef]
7. Shi, Q.; Qin, Z.; Xu, H.; Li, G. Heterogeneous Cross-Coupling over Gold Nanoclusters. *Nanomaterial* **2019**, *9*, 838. [CrossRef]
8. Zhang, C.; Chen, Y.; Wang, H.; Li, Z.; Zheng, K.; Li, S.; Li, G. Transition-Metal-Mediated Catalytic Properties of CeO_2-Supported Gold Clusters in Aerobic Alcohol Oxidation. *Nano Res.* **2018**, *11*, 2139–2148. [CrossRef]
9. Chen, Y.; Li, Y.; Chen, W.; Xu, W.W.; Han, Z.-k.; Waheed, A.; Ye, Z.; Li, G.; Baiker, A. Continuous Dimethyl Carbonate Synthesis from CO2 and Methanol over $Bi_xCe_{1-x}O\delta$ Monoliths: Effect of Bismuth Doping on Population of Oxygen Vacancies, Activity, and Reaction Pathway. *Nano Res.* **2022**, *15*, 1366–1374. [CrossRef]
10. Shi, Q.; Qin, Z.; Sharma, S.; Li, G. Recent progress in heterogeneous catalysis over atomically and structurally precise metal nanoclusters. *Chem. Rec.* **2021**, *21*, 879–892. [CrossRef] [PubMed]
11. Sargazi, S.; Laraib, U.; Er, S.; Rahdar, A.; Hassanisaadi, M.; Zafar, M.N.; Diez-Pascual, A.M.; Bilal, M. Application of Green Gold Nanoparticles in Cancer Therapy and Diagnosis. *Nanomaterials* **2022**, *12*, 1102. [CrossRef] [PubMed]
12. Abed, J.; Rajput, N.S.; El Moutaouakil, A.; Jouiad, M. Recent Advances in the Design of Plasmonic Au/TiO_2 Nanostructures for Enhanced Photocatalytic Water Splitting. *Nanomaterials* **2020**, *10*, 2260. [CrossRef] [PubMed]
13. Zhang, H.; Chen, G.; Bahnemann, D.W. Photoelectrocatalytic materials for environmental applications. *J. Mater. Chem.* **2009**, *19*, 5089–5121. [CrossRef]
14. Kiss, J.; Sapi, A.; Toth, M.; Kukovecz, A.; Konya, Z. Rh-induced Support Transformation and Rh Incorporation in Titanate Structures and Their Influence on Catalytic Activity. *Catalysts* **2020**, *10*, 212. [CrossRef]
15. Patial, S.; Hasija, V.; Raizada, P.; Singh, P.; Singh, A.A.P.K.; Asiri, A.M. Tunable photocatalytic activity of $SrTiO_3$ for water splitting: Strategies and future scenario. *J. Environ. Chem. Eng.* **2020**, *8*, 103791. [CrossRef]
16. Xia, C.; Nguyen, T.H.C.; Nguyen, X.C.; Kim, S.Y.; Nguyen, D.L.T.; Raizada, P.; Singh, P.; Nguyen, V.-H.; Nguyen, C.C.; Hoang, V.C.; et al. Emerging cocatalysts in TiO_2-based photocatalysts for light-driven catalytic hydrogen evolution: Progress and perspectives. *Fuel* **2022**, *307*, 121745. [CrossRef]
17. Raza, A.; Altaf, S.; Ali, S.; Ikram, M.; Li, G. Recent Advances in Carbonaceous Sustainable Nanomaterials for Wastewater Treatments. *Sustain. Mater. Technol.* **2022**, *32*, e00406. [CrossRef]
18. Raizada, P.; Sudhaik, A.; Patial, S.; Hasija, V.; Khan, A.A.P.; Singh, P.; Gautam, S.; Kaur, M.; Nguyen, V.-H. Engineering nanostructures of CuO-based photocatalysts for water treatment: Current progress and future challenges. *Arab. J. Chem.* **2020**, *13*, 8424–8457. [CrossRef]
19. Wang, Y.; Zhang, Y.; Jiang, Q.; Guo, S.; Baiker, A.; Li, G. Ternary CuCrCeOx Solid Solution Enhances N_2-Selectivity in the NO Reduction with CO in the Presence of Water and Oxygen. *ChemCatChem* **2022**, *14*, e202200203.
20. Wang, Y.; Jiang, Q.; Xu, L.; Han, Z.-K.; Guo, S.; Li, G.; Baiker, A. Effect of Configuration of Copper Oxide-Ceria Catalysts in NO Reduction with CO: Superior Performance of Copper-Ceria Solid Solution. ACS Appl. *Mater. Interfaces* **2021**, *13*, 61078–61087. [CrossRef]
21. Shi, Q.; Wang, Y.; Guo, S.; Han, Z.-K.; Ta, N.; Li, G.; Baiker, A. NO reduction with CO over $CuOx/CeO_2$ Nanocomposites: Influence of Oxygen Vacancies and Lattice Strain. *Catal. Sci. Technol.* **2021**, *11*, 6543–6552. [CrossRef]

22. Liu, J.L.; Zhan, E.S.; Cai, W.J.; Li, J.; Shen, W.J. Methanol Selective Oxidation to Methyl Formate over ReO_x/CeO_2 Catalysts. *Catal. Lett.* **2008**, *120*, 274–280. [CrossRef]
23. Kaiser, D.; Beckmann, L.; Walter, J.; Bertau, M. Conversion of Green Methanol to Methyl Formate. *Catalysts* **2021**, *11*, 869. [CrossRef]
24. Shi, Q.; Wei, X.; Raza, A.; Li, G. Recent Advances in Aerobic Photo-Oxidation of Methanol to Valuable Chemicals. *ChemCatChem* **2021**, *13*, 3381–3395. [CrossRef]
25. Zhang, Y.; Cao, C.; Li, G. Recent Progress in Green Conversion of Biomass Alcohol to Chemicals via Aerobic Oxidation. *Biomass* **2022**, *2*, 103–115. [CrossRef]
26. Shi, Q.Q.; Ping, G.C.; Wang, X.J.; Xu, H.; Li, J.M.; Cui, J.Q.; Abroshan, H.D.; Ding, H.J.; Li, G. CuO/TiO_2 heterojunction composites: An efficient photocatalyst for selective oxidation of methanol to methyl formate. *J. Mater. Chem. A* **2019**, *7*, 2253–2260. [CrossRef]
27. Wittstock, A.; Zielasek, V.; Biener, J.; Friend, C.M.; Bäumer, M. Nanoporous Gold Catalysts for Selective Gas-Phase Oxidative Coupling of Methanol at Low Temperature. *Science* **2010**, *327*, 319–322. [CrossRef]
28. Raza, A.; Zhang, X.; Ali, S.; Cao, C.; Rafi, A.A.; Li, G. Photoelectrochemical Energy Conversion over 2D Materials. *Photochem* **2022**, *2*, 272–298. [CrossRef]
29. Liu, J.; Han, C.H.; Yang, X.Z.; Gao, G.J.; Shi, Q.Q.; Tong, M.; Liang, X.Y.; Li, C.F. Methyl formate synthesis from methanol on titania supported copper catalyst under UV irradiation at ambient condition: Performance and mechanism. *J. Catal.* **2016**, *333*, 162–170. [CrossRef]
30. Guo, S.; Zhang, S.H.; Fang, Q.H.; Abroshan, H.D.; Kim, H.; Haruta, M.; Li, G. Gold-Palladium Nanoalloys Supported by Graphene Oxide and Lamellar TiO_2 for Direct Synthesis of Hydrogen Per-oxide. *ACS Appl. Mater. Interfaces* **2018**, *10*, 40599–40607. [CrossRef]
31. Kollhoff, F.; Schneider, J.; Li, G.; Sami, B.; Shen, W.J.; Berger, T.; Diwald, O.; Libuda, J. Anchoring of carboxyl-functionalized porphyrins on MgO, TiO_2, and Co_3O_4 nanoparticles. *Phys. Chem. Chem. Phys.* **2018**, *20*, 24858–24868. [CrossRef]
32. Shao, B.; Zhao, W.N.; Miao, S.; Huang, J.H.; Wang, L.L.; Li, G.; Shen, W.J. Facet-dependent anchoring of gold nanoparticles on TiO_2 for CO oxidation. *Chin. J. Catal.* **2019**, *40*, 1534–1539. [CrossRef]
33. Waheed, A.; Shi, Q.; Maeda, N.; Meier, D.M.; Qin, Z.; Li, G.; Baiker, A. Strong Activity Enhancement of the Photocatalytic Degradation of an Azo Dye on Au/TiO_2 Doped with FeO_x. *Catalysts* **2020**, *10*, 933. [CrossRef]
34. Shi, Q.Q.; Qin, Z.X.; Yu, C.L.; Waheed, A.; Xu, H.; Gao, Y.; Abroshan, H.; Li, G. Experimental and mechanistic understanding of photo-oxidation of methanol catalyzed by CuO/TiO_2-spindle nano-composite: Oxygen vacancy engineering. *Nano Res.* **2020**, *13*, 939–946. [CrossRef]
35. Zhang, S.; Gong, X.; Shi, Q.; Ping, G.; Xu, H.; Waleed, A.; Li, G. CuO Nanoparticle-Decorated TiO_2-Nanotube Heterojunctions for Direct Synthesis of Methyl Formate via Photo-Oxidation of Methanol. *ACS Omega* **2020**, *5*, 15942–15948. [CrossRef]
36. Fang, Q.; Qin, Z.; Shi, Y.; Liu, F.; Barkaoui, S.; Abroshan, H.; Li, G. Au/NiO Composite: A Catalyst for One-Pot Cascade Conversion of Furfural. *ACS Appl. Energy Mater.* **2019**, *2*, 2654–2661. [CrossRef]
37. Liu, C.; Zhang, J.; Huang, J.; Zhang, C.; Hong, F.; Zhou, Y.; Li, G.; Haruta, M. Efficient Aerobic Oxidation of Glucose to Gluconic Acid over Activated Carbon-Supported Gold Clusters. *ChemSuSChem* **2017**, *10*, 1976–1980. [CrossRef]
38. Zheng, K.; Zhang, J.; Zhao, D.; Yang, Y.; Li, Z.; Li, G. Motif Mediated $Au_{25}(SPh)_5(PPh_3)_{10}X_2$ Nanorod of Conjugated Electron Delocalization. *Nano Res.* **2019**, *12*, 501–507. [CrossRef]
39. Qin, Z.; Sharma, S.; Wan, C.-Q.; Malola, S.; Xu, W.-W.; Häkkinen, H.; Li, G. A Homoleptic Alkynyl-Ligated $[Au_{13}Ag_{16}L_{24}]^{3-}$ Cluster as a Catalytically Active Eight-Electron Superatom. *Angew. Chem. Int. Ed.* **2020**, *59*, 970–975.
40. Qin, Z.; Zhang, J.; Wan, C.-Q.; Liu, S.; Abroshan, H.; Jin, R.; Li, G. Atomically Precise Nanoclusters with Reversible Isomeric Transformation for Rotary Nanomotors. *Nat. Commun.* **2020**, *11*, 6019. [CrossRef]
41. Qin, Z.; Hu, S.; Han, W.; Li, Z.; Xu, W.W.; Zhang, J.; Li, G. Tailoring optical and photocatalytic properties by single-Ag-atom exchange in $Au_{13}Ag_{12}(PPh_3)_{10}Cl_8$ nanoclusters. *Nano Res.* **2022**, *15*, 2971–2976. [CrossRef]
42. Zhu, H.; Yuan, X.; Yao, Q.; Xie, J. Shining photocatalysis by gold-based nanomaterials. *Nano Energy* **2021**, *88*, 106306. [CrossRef]
43. Li, W.; Liu, C.; Abroshan, H.; Ge, Q.; Yang, X.; Xu, H.; Li, G. Catalytic CO Oxidation Using Bimetallic M_xAu_{25-x} Clusters: A Combined Experimental and Computational Study on Doping Effects. *J. Phys. Chem. C* **2016**, *120*, 10261–10267. [CrossRef]
44. Gong, X.; Zhang, X.; Shi, Q.; Li, J.; Ping, G.; Xu, H.; Ding, H.; Li, G. Synergistic Effects of $PtFe/CeO_2$ Catalyst afford high Catalytic Performance in selective hydrogenation of cinnamaldehyde. *J. Rare Earths* 2022, *in press*. [CrossRef]
45. Du, X.; Huang, Y.; Pan, X.; Han, B.; Su, Y.; Jiang, Q.; Li, M.; Tang, H.; Li, G.; Qiao, B. Size-dependent strong metal-support interaction in TiO_2 supported Au nanocatalysts. *Nat. Commun.* **2020**, *11*, 5811. [CrossRef]
46. Shi, Y.; Tian, S.; Shi, Q.; Waheed, A.; Cao, Y.; Li, G. Cascade aldol condensation of an aldehyde via the aerobic oxidation of ethanol over an Au/NiO composite. *Nanoscale Adv.* **2019**, *1*, 3654–3659. [CrossRef]
47. Mallat, T.; Baiker, A. Potential of Gold Nanoparticles for Oxidation in Fine Chemical Synthesis. *Annu. Rev. Chem. Biomol.* **2012**, *3*, 11–28. [CrossRef]
48. Naya, S.; Kimura, K.; Tada, H. One-Step Selective Aerobic Oxidation of Amines to Imines by Gold Nanoparticle-Loaded Rutile Titanium(IV) Oxide Plasmon Photocatalyst. *ACS Catal.* **2013**, *3*, 10–13. [CrossRef]
49. Qin, Z.; Wang, J.; Sharma, S.; Malola, S.; Wu, K.; Häkkinen, H.; Li, G. Photo-Induced Cluster-to-Cluster Transformation of $[Au_{37-x}Ag_x(PPh_3)_{13}Cl_{10}]^{3+}$ into $[Au_{25-y}Ag_y(PPh_3)_{10}Cl_8]^{+}$: Fragmentation of A Trimer of 8-Electron Superatoms by Light. *J. Phys. Chem. Lett.* **2021**, *12*, 10920–10926. [CrossRef] [PubMed]

50. Chen, Q.; Qin, Z.; Liu, S.; Zhu, M.; Li, G. On the Redox Property of Ag16Au13 Clusters and Its Catalytic Application in the Photooxidation. *J. Chem. Phys.* **2021**, *154*, 164308. [CrossRef]
51. Chen, H.; Liu, C.; Wang, M.; Zhang, C.; Luo, N.; Wang, Y.; Abroshan, H.; Li, G.; Wang, F. Visible Light Gold Nanocluster Photocatalyst: Selective Aerobic Oxidation of Amines to Imines. *ASC Catal.* **2017**, *7*, 3632–3638. [CrossRef]
52. Liu, C.; Abroshan, H.; Yan, C.; Li, G.; Haruta, M. One-pot synthesis of $Au_{11}(PPh_2Py)_7Br_3$ for the highly chemoselective hydrogenation of nitrobenzadehyde. *ACS Catal.* **2016**, *6*, 92–99. [CrossRef]
53. Chen, Y.; Liu, C.; Abroshan, H.; Wang, J.; Li, Z.; Li, G.; Haruta, M. Phosphine/Phenylacetylide-Ligated Au Cluster for Multicomponent Coupling Reaction. *J. Catal.* **2016**, *337*, 287–294. [CrossRef]
54. Qin, Z.; Zhao, D.; Zhao, L.; Xiao, Q.; Wu, T.; Zhang, J.; Wan, C.; Li, G. Tailoring the Stability, Photocatalysis and Photoluminescence Properties of Au_{11} Nanocluster via Doping Engineering. *Nanoscale Adv.* **2019**, *1*, 2529–2536. [CrossRef]
55. Mulliken, R.S. Interpretation of the Atmospheric Oxygen Bands; Electronic Levels of the Oxygen Molecule. *Nature* **1928**, *122*, 505. [CrossRef]
56. Jin, R. Atomically precise metal nanoclusters: Stable sizes and optical properties. *Nanoscale* **2015**, *7*, 1549. [CrossRef]
57. Kawasaki, H.; Kumar, S.; Li, G.; Zeng, C.; Kauffman, D.R.; Yoshimoto, J.; Iwasaki, Y.; Jin, R. Generation of singlet oxygen by photoexcited $Au_{25}(SR)_{18}$ clusters. *Chem. Mater.* **2014**, *26*, 2777–2788. [CrossRef]
58. Hayyan, M.; Hashim, M.A.; AlNashef, I.M. Superoxide Ion: Generation and Chemical Implications. *Chem. Rev.* **2016**, *116*, 3029–3085. [CrossRef]
59. Li, Z.; Liu, C.; Abroshan, H.; Kauffman, D.R.; Li, G. $Au_{38}S_2(SAdm)_{20}$ Photocatalyst for One-Step Selective Aerobic Oxidations. *ACS Catal.* **2017**, *7*, 3368–3374. [CrossRef]
60. Liu, C.; Yan, C.; Lin, J.; Yu, C.; Huang, J.; Li, G. One-Pot Synthesis of $Au_{144}(SCH_2Ph)_{60}$ Nanoclusters and Catalytic Application. *J. Mater. Chem. A* **2015**, *3*, 20167–20173. [CrossRef]
61. Wang, C.; Astruc, D. Nanogold plasmonic photocatalysis for organic synthesis and clean energy conversion. *Chem. Soc. Rev.* **2014**, *43*, 7188–7216. [CrossRef] [PubMed]
62. Zhang, J.; Zhou, Y.; Zheng, K.; Abroshan, H.; Kauffman, D.R.; Sun, J.; Li, G. Diphosphine-induced chiral propeller arrangement of gold nanoclusters for singlet oxygen photogeneration. *Nano Res.* **2018**, *11*, 5787–5798. [CrossRef]
63. Waheed, A.; Cao, C.; Zhang, Y.; Zheng, K.; Li, G. Insight into Au/ZnO Catalyzed Aerobic Benzyl Alcohol Oxidation by Modulation-Excitation Attenuated Total Reflection IR Spectroscopy. *New J. Chem.* **2022**, *46*, 5361–5367. [CrossRef]
64. Shi, Q.; Zhang, X.; Liu, X.; Xu, L.; Liu, B.; Zhang, J.; Xu, H.; Han, Z.; Li, G. In-situ exfoliation and assembly of 2D/2D g-C_3N_4/TiO_2(B) hierarchical microflower: Enhanced photo-oxidation of benzyl alcohol under visible light. *Carbon* **2022**, *195*, 401–409. [CrossRef]
65. Zhang, X.; Shi, Q.; Liu, X.; Li, J.; Xu, H.; Ding, H.; Li, G. Facile assembly of InVO4/TiO_2 heterojunction for enhanced photo-oxidation of benzyl alcohol. *Nanomaterials* **2022**, *12*, 1544. [CrossRef]
66. Shi, Q.; Raza, A.; Xu, L.; Li, G. Bismuth oxyhalide quantum dots modified titanate-necklaces with exceptional population of oxygen vacancies and photocatalytic activity. *J. Colloid Interface Sci.* **2022**, *625*, 750–760. [CrossRef]
67. Cao, Y.; Su, Y.; Xu, L.; Yang, X.; Han, Z.; Cao, R.; Li, G. Ionic liquids modified oxygen vacancy-rich amorphous FeNi hydroxide nanoclusters on carbon-based materials as an efficient electrocatalyst for electrochemical water oxidation. *J. Energy Chem.* **2022**, *71*, 167–173. [CrossRef]
68. Cao, Y.; Guo, S.; Yu, C.; Zhang, J.; Pan, X.; Li, G. Ionic liquid-assisted one-step preparation of ultrafine amorphous metallic hydroxide nanoparticles for the highly efficient oxygen evolution reaction. *J. Mater. Chem. A* **2020**, *8*, 15767–15773. [CrossRef]
69. Liu, Z.; Qin, Z.; Cui, C.; Luo, Z.; Yang, B.; Jiang, Y.; Lai, C.; Wang, Z.; Wang, X.; Fang, X.; et al. In-Situ Generation and Global Property Profiling of Metal nanoclusters by Ultraviolet Laser Dissociation-Mass Spectrometry. *Sci. China Chem.* **2022**, 65. [CrossRef]
70. Raza, A.; Ikram, M.; Guo, S.; Baiker, A.; Li, G. Green Synthesis of Dimethyl Carbonate from CO_2 and Methanol: New Strategies and Industrial Perspective. *Adv. Sustain. Syst.* **2022**, *6*, 2200087. [CrossRef]
71. Zhang, X.; Li, Z.; Pei, W.; Li, G.; Liu, W.; Du, P.; Wang, Z.; Qin, Z.; Qi, H.; Liu, X.; et al. Crystal Phase Mediated Restructuring of Pt on TiO_2 with Tunable Reactivity: Redispersion versus Reshaping. *ACS Catal.* **2022**, *12*, 3634–3643. [CrossRef]
72. Zhang, S.; Zhang, B.; Li, Z.; Yang, X.; Meng, F.; Liang, H.; Lei, Y.; Wu, H.; Zhang, J.; Li, G.; et al. Surface Isolation of Single Metal complexes or Clusters by a Coating Sieving Layer via Atomic Layer Deposition. *Cell Rep. Phys. Sci.* **2022**, *3*, 100787. [CrossRef]